Development of a superconducting elliptically polarized undulator

2010 J. Phys.: Conf. Ser. 234 032006

(http://iopscience.iop.org/1742-6596/234/3/032006)

Development of a superconducting elliptically polarized undulator

S D Chen[1], J C Jan[2], C S Hwang[2] and K S Liang[1,2]

[1]Department of of Electrophysics, National Chiao Tung University, Hsinchu 300, Taiwan
[2]NSRRC, 101 Hsin-Ann Road, Hsinchu Science Park, Hsinchu 30076, Taiwan

E-mail: cshwang@nsrrc.org.tw

Abstract. A superconducting, elliptically polarized undulator (SEPU24) with a period of length 24 mm was developed to provide first-harmonic photons from a 0.8 GeV storage ring for extreme-ultraviolet (EUV) lithography experiment. In SEPU24, two layers of a magnet array structure – with and without rotated magnet arrays – are combined to generate a helical field that provides radiation with wavelength 13.5 nm in the in-band energy. The arrays of iron and aluminium poles were wound with a racetrack coil vertically as for the magnet pole array. The elliptical field is created when the up and down magnet-pole arrays pass excitation currents in alternate directions. SEPU24 is designed with a magnet of gap 6.8 mm, yielding magnetic flux density B_x=B_z=0.61 T of the helical field. A prototype magnet was fabricated with a diode for quench protection, and assembled in a test dewar to test the magnet performance. A cryogenic Hall-probe system with a precise linear stage was used to measure the distribution of the magnetic field. We describe the design concept and algorithm, the engineering design, the calculation of the magnetic field, the construction and testing of the 10-pole prototype magnet and related issues.

1. Introduction

The electron energy of the Taiwan light source (TLS, NSRRC) will be altered to 0.8-1 GeV when the Taiwan Photon Source (TPS) becomes routinely operational. We will therefore develop a superconducting elliptically polarized undulator (SEPU) for 0.8 GeV TLS for a coherent harmonic-generation (CHG) free-electron laser (FEL) in a circular-polarization mode. The power radiated from the circular polarization mode will concentrate in the in-band range at wavelength 13.5 nm [1].

Several schemes [2-10] have been developed to generate the helically distributed fields; they involve electromagnets with copper coils, and hybrid or pure structures with permanent magnets in various configurations. Such schemes involve a planar geometry with a variable phase and can yield variably polarized light; the elliptically polarized undulator device *APPLE II* is especially effective, but the magnetic-flux density is invariably less than that of a superconducting elliptically polarized undulator.

Here we describe a superconducting elliptically polarized undulator [11] with a period of length 24 mm to produce a helical field in the FEL photon source that can be operated at the accelerator facilities of the storage ring, the linear accelerator and the energy-recovery linear accelerator (ERL). Such a magnet provides intense light that is right- and left-circularly polarized, and can generate also linearly polarized light in the horizontal and vertical directions [8]. Combining an inner magnet array with an unrotated iron pole and an outer magnet array with a rotated aluminum pole creates various polarizations on varying the excitation current in the two layers. The circular-polarization mode possesses a feature that only the fundamental frequency is obtained; the total radiation power is thereby constrained to the in-band region in the EUV lithography experiment [1], and the heat load on the beam line mirror is hence much less than that in the linear- or elliptical-polarization mode. Two independent power supplies are used to excite the polarization switching for right- and left-elliptically polarized radiation as well as linear polarization that might also be used in the EUV source. One 10-pole prototype SEPU24 was designed and fabricated to assess the feasibility of application of an elliptically polarized undulator for EUV lithography. A system to measure the field was developed, and a vertical test Dewar was planned for that field measurement and magnet testing. The features of the magnetic field of the SEPU24 have been elucidated.

2. Design concept of the switching polarization mechanism

The design concept of SEPU24 is to combine two magnet arrays as depicted schematically in Figure 1. Two planar magnet arrays with periods of the same length, 24 mm, comprise a superconducting, elliptically polarized undulator structure.

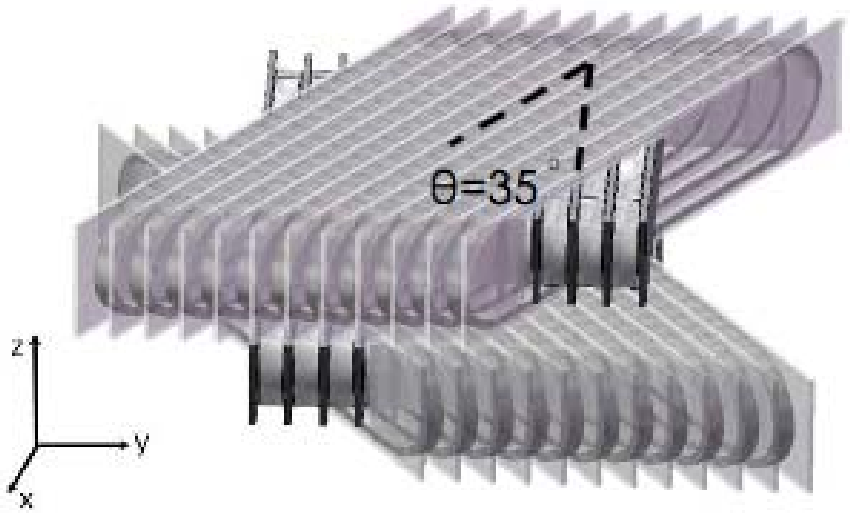

Figure 1. Schematic layout of inner and outer magnet arrays combined as an elliptically polarized undulator.

The outer magnet array has a pole that is rotated [8,11] through 35° while the inner magnet array has a fixed pole. When the up and down magnetic-pole arrays are parallel, like the inner magnet array, a vertical magnetic field is generated. The magnetic-flux density in three components, B_x, B_y and B_z, delivers the sinusoidal field in the longitudinal y-axis that is contributed by the up and down magnetic pole arrays without rotation of the pole ($\theta=0^o$) according to equations (1)-(3) [8], which fully express the magnetic-field components near the axis in the racetrack-coil structure:

$$B_z = B_{z0}\cosh(\varphi_z z)\cosh(\varphi_x x)\cos(\varphi_0 y) \quad (1)$$

$$B_x = -\frac{\varphi_x}{\varphi_z}B_{z0}\sinh(\varphi_z z)\sinh(\varphi_x x)\cos(\varphi_0 y) \quad (2)$$

$$B_y = -\frac{\varphi_0}{\varphi_z}B_{z0}\sinh(\varphi_z z)\cosh(\varphi_x x)\sin(\varphi_0 y) \quad (3)$$

in which $\varphi_x^2 + \varphi_z^2 = \varphi_0^2 = (2\pi/\lambda_u)^2$ and λ_u represents the periodic length; Bz0 is generated by an exciting current in the superconducting coil.

If the up and down magnetic-pole arrays of the planar undulator are rotated by angle θ in the horizontal plane, by means of the outer magnet array, the on-axis ($x=z=0$) elliptical field is expressed approximately according to equations (4)-(5) [8],

$$B_z(y) = B_{z0}\cos(2\pi y/\lambda_u) \quad (4)$$

$$B_x(y) = B_y \sin\theta = -\frac{\varphi_0}{\varphi_z}B_{z0}\sin(2\pi y/\lambda_u)\sin\theta \quad (5)$$

According to Eqs. (4) and (5), the two transverse fields B_x and B_z are out of phase and so generate elliptically polarized radiation. The two magnet arrays are combined as in Figure 1. This arrangement is optimized for the circular-polarization mode as it maximizes the field strength of the helical fields

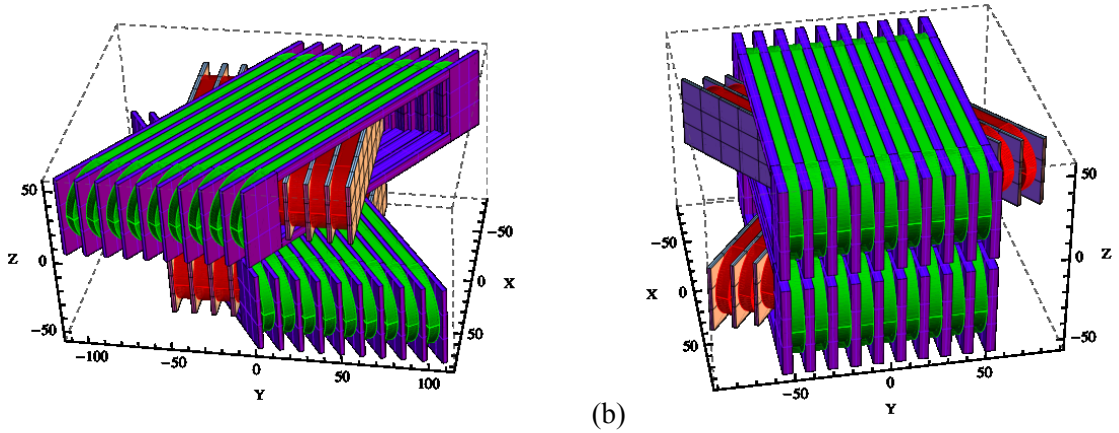

Figure 2. (a) The 3d magnetic structure used in Radia for the simulations. (b) The rotated and unrotated pole of the inner and outer magnet array was interchanged.

Table 1. Combination of excitation currents for various polarization modes of the superconducting elliptically polarized undulator. Six polarization modes exist that are operated with electron energy 0.8 GeV: right elliptical polarization (REP), left elliptical polarization (LEP), right circular polarization (RCP), left circular polarization (LCP), vertical polarization (VP) and horizontal polarization (HP).

	REP	LEP	RCP	LCP	VP	HP
excitation current J_o (J_i) /A mm^{-2}	1073 (0)	340 (-1021)	1073 (-1021)	281 (-1021)	446 (-1021)	0 (-1021)
magnetic-flux density B_z (B_x) /T	1.038 (0.605)	-0.103 (0.192)	0.606 (0.606)	-0.157 (0.157)	0 (0.252)	-0.429 (0)

B_z and B_x. When a higher harmonic spectrum is required, the rotated and unrotated poles of the inner and outer magnet array should be interchanged (Figure 2(b)). Under such a change of magnet array, the magnetic-flux density in the elliptical- or linear-polarization mode increases. Excitation currents J_i and J_o in the inner and outer arrays of the superconducting coils are mutually independent.

In this structure, the polarization is switchable using various combinations of excitation currents J_i and J_o. The pole materials of the outer and inner magnetic arrays are aluminum and low-carbon steel, respectively. The polarization modes are varied with the combination of the two excitation currents. Table 1 lists the features of polarization modes of six types. Our purpose is concentrated on the type RCP that is the circularly polarized mode for EUV lithography. The types LEP, VP and LCP are ineffective for a magnet array of this arrangement, except the structure shown in Figure 2(b) was used. The RCP field generated with an Apple-II structure was simulated with the same period length and gap; the RCP field strength with SEPU is two times greater than with Apple II EPU (B_x=B_z=0.3 T).

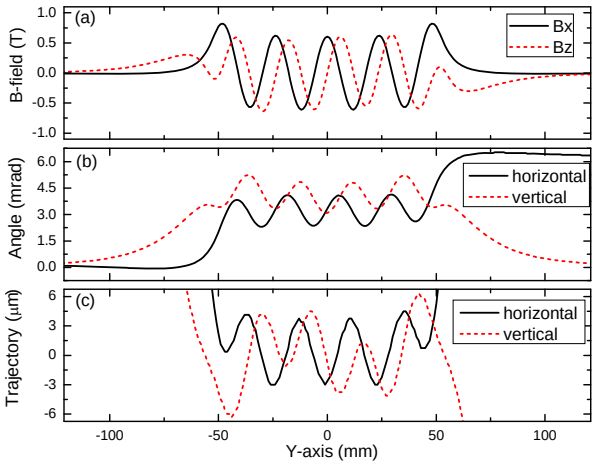

Figure 3. (a)The circular polarized field distribution on longitudinal axis of on-axis magnetic field was calculated at the excitation current of 457.5 and 435.4 A in the outer and inner magnet array, respectively. The first and second integral field of the calculated field were also shown in (b) and (c), respectively.

Table 2. Principal design parameters of SEPU24 in the circular-polarization mode

number of poles	10
coil cross-section of inner, outer array /mm^2	9.02 × 6.76, 6.56 × 3.64
periodic length λ_u /mm	24
magnet gap *g* of inner, outer arrays /mm	19.08, 6.8
rotation angles of inner, outer poles with /deg	0, -35
maximum field B_s on inner, outer coils /T	4.15, 3.54
excitation current I_i , I_o /A	-435.4, 457.5
excitation current densities J_i, J_o /A mm^{-2}	-1021, 1073
field strength B_z=B_x /T	0.606
total energy /kJ	8.513
force between upper and lower magnet arrays $\{F_x,F_y,F_z\}$ /kg	{0.1,-0.3, -102.6}
torque between upper and lower magnet arrays $\{T_x,T_y,T_z\}$ /kg cm	{2.28, -0.75, -287.2}
force between inner and outer magnet arrays $\{F_x,F_y,F_z\}$ /kg	{0, -0.1, 0.1}
torque between inner and outer magnet arrays $\{T_x,T_y,T_z\}$ /kg cm	{0.05, 0.16, 1205.6}

3. Design And Analysis Of Magnet

The SEPU24 is designed to be operated in the circular-polarization mode. The magnetic field was simulated with Radia program code [12]. The helical field is generated with the superposition of fields from the rotated and unrotated magnet arrays; Figure 2(a) shows the magnetic structure used in Radia for the simulations. To decrease the interaction between the fields from the inner and outer magnet arrays and to enhance the field strength, an iron inner pole and an aluminum outer pole were used. Based on this SEPU24 structure, the magnetic circuit of a 10-pole magnet array was designed, and the field features were calculated. Figure 3 (a) shows results of the simulation for which the phase difference between B_x and B_z is $\pi/2$ and the field strengths B_x and B_z are equal. The first ($\int B\,dy$) and second ($\iint B\,dy\,dy'$) field integrals, representing the electron angle and the trajectory of the moving electrons, are shown in Figure 3(b) and (c). As the end pole is not optimized in the calculation model, two virtual correctors serve to adjust the angle and trajectory.

Table 2 lists the magnet design parameters of SEPU24. The period length was 24 mm; the magnet air gaps in the inner and outer arrays were *19.08* and *6.8* mm, respectively. Superconducting NbTi rectangular wire was used to wind the coil. Table 3 presents the specifications and the characteristics of the superconducting rectangular wire. The peak field B_s on the inner and outer coils was maximal under a helical-polarization condition, at *4.15 T* and *3.54 T*, respectively. According to these data, the safety margin for the current density in the magnet design, which is defined as the design current divided by the critical current, was 98 %. The roll-off ($\Delta B(x)/B(0)$) and integral field ($\int B(x)\,dy$) in the circular-polarization mode were investigated. Figure 4(a) reveals the calculated field distribution of roll-off in the circular-polarization mode that had been out of the specification ($\Delta B/B=0.5\%$ *at* $x=\pm 10$

Table 3. Specifications and characteristics of conductor in SEPU magnet

Cu/SC ratio	1.35
Twist pitch (mm)	26±2
Peak field B_s of short sample @450A (T)	4.2
Bare dimensions (mm^2)	0.46×0.72
Dimensions including insulation (mm^2)	0.51×0.77
Filament size (μm)	54
Number of filaments	54
R.R.R.	70

mm). The rapid decay of roll-off on the transverse axis is the critical issue for SEPU alignment and the top-up injection operation in the storage ring. Figure 4(b) shows the results of analysis of the integral field strength existing in the multipole field strength in the circular-polarization mode. Slight quadrupole and sextupole components in the vertical and horizontal fields, respectively, occurred when the operation mode was fixed at the circular-polarization mode. Multipole correctors [13] were accordingly required at both ends of the SEPU24 to compensate the multipole field components and to adjust the first ($\int B\,dy$) and second ($\iint B\,dy\,dy'$) field integrals to be lower than the specification of 20 G cm and 5000 G cm^2, respectively. Figure 5 is a plot of the total energy and inductance as functions of excitation current. The total maximum energy of this magnet was 8.51 kJ that will serve as a reference for the circuit design for quenching protection. The energy and inductance in Figure 5(a) are excited by only J_o; Figure 5(b) shows the combination of currents J_o and J_i.

To understand the stability of the mechanical support we analyzed the three-dimensional magnetic force between the two magnet arrays. Table 2 lists the force and torque between the magnet arrays of the inner and outer and the upper and lower, respectively. The three components of force and torque

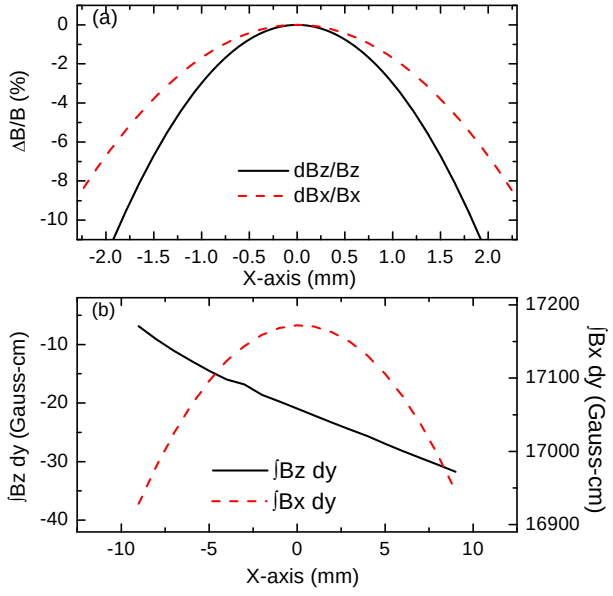

Figure 4. (a) roll-off and (b) integral field deviation along transverse axis in the circular polarization mode (without optimization of the end pole).

Table 4. Calculation of force and stress on coil

pos.	force /kg	stress /psi
	outer layer coil	
1	(F_x= -0.1, F_y= -0.1, F_z= 13.6)	(S_x= 0.45 , S_y=0.32 , S_z=20.7)
2	(F_x= -0.2, F_y= -0.1, F_z= -8.0)	(S_x= 0.90 , S_y= 0.32, S_z=12.2)
3	(F_x= 35.2, F_y= 18.7, F_z= -5.0)	(S_x= 148.5, S_y=97.5 , S_z=42.2)
4	(F_x= -35.0, F_y= -18.7, F_z= -5.1)	(S_x= 147.6, S_y=97.5 , S_z=43.1)
	inner layer coil	
1	(F_x= -0.5 , F_y= 0.1 , F_z= -312.8)	(S_x= 11.7 , S_y=0.26 , S_z=616.6)
2	(F_x= -0.6 , F_y= 0.14, F_z= 301.7)	(S_x= 14.0 , S$_y$=0.37 , S_z=594.7)
3	(F_x= -206.1, F_y= 4.5 , F_z= 6.9)	(S_x= 830.8, S_y=18.7 , S_z= 55.9)
4	(F_x= 205.7, F_y= -3.6 , F_z= 6.7)	(S_x= 829.1, S_y= 15.0, S_z= 54.3)

are negligible except along the vertical axis. The vertical torque and force between the magnet array of the inner and outer are controlled by tight contacting and with an aluminum fixture block between the outer and inner magnet arrays. Table 2 indicates that the torque between the upper and lower magnet arrays is larger on the vertical axis than elsewhere. An aluminum supporting bar and fixture between the upper and lower arrays serves to overcome the torque. For the analysis of the coil stress, each racetrack was divided into four parts in Figure 6 that also presents the coil dimension to analyze the force and stress on it [14]. This analysis will aid our understanding of the coil design whether it can work reliably.

Table 4 lists the results of analyses of the magnet force and stress on the parts of the local coils. The attractive force of the outer layer coil was maximal at the locally curved part. The curved part of the conductor that is semi-circular and symmetrical was impregnated with epoxy to enable the force to be supported. The force on the straight part of the racetrack coil was an attraction to the pole; the force and stress were also shown in Table 4. The attractive force of the inner layer coil was maximal at the straight-line part. The analyzed stresses at each coil part are not critical for the reinforcement epoxy.

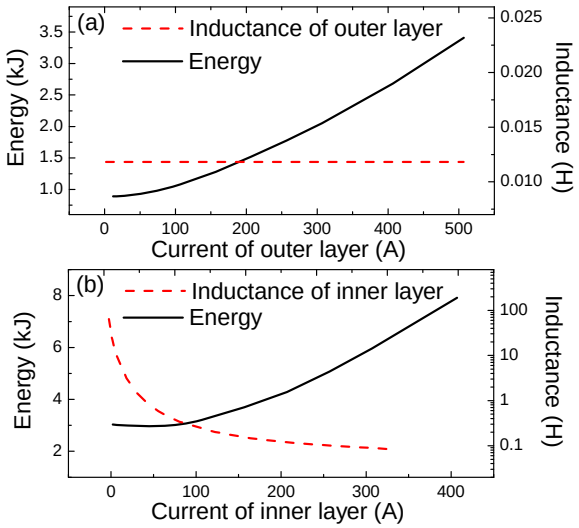

Figure 5. Total energy and inductance as functions of excitation current such that (a) the excitation current was charged with only the outer layer coil, and (b) outer layer coil was fixed at 500 A and the inner layer current was excited simultaneously.

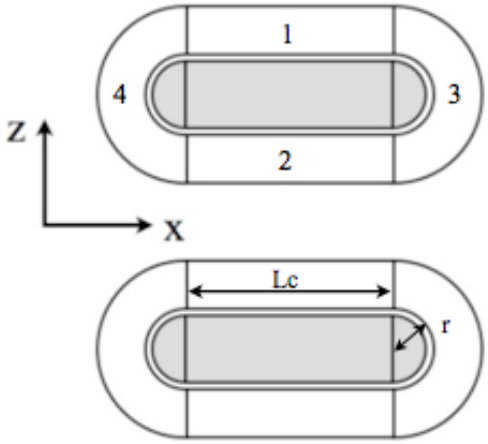

Figure 6. Locations of forces and stress calculation of the conductor divided into four parts. For the inner magnet array, L_c=80 mm, r=12.6 mm; for the outer magnet array, L_c=142 mm, r=21.8 mm; their cross sections are shown in Table 2.

As a precise assembly of the two magnet arrays was crucial for the magnetic-field performance; a reference fixture was adopted to assemble the two magnet arrays at the exact relative longitudinal position.

4. 10-Pole Prototype Test

The 10-pole prototype was constructed, assembled and tested in a vertical test Dewar. Figure 7(a) and (b) present photographs of the separated inner and outer magnet arrays; Figure 7(c) shows the 10-pole prototype assembled with the inner and outer magnet arrays. A cryogenic-Hall probe, associated with a rail guider that was assembled with the 10-pole prototype and inserted into the vertical test Dewar, was used to measure the distribution of magnet field on the axis. The two magnet arrays have independent power supplies. A diagram of the power supply connected with the quench protection circuit and the superconducting coil appears in Figure 8. The upper and lower magnet arrays are connected in series. 1000-A current leads were used in this system.

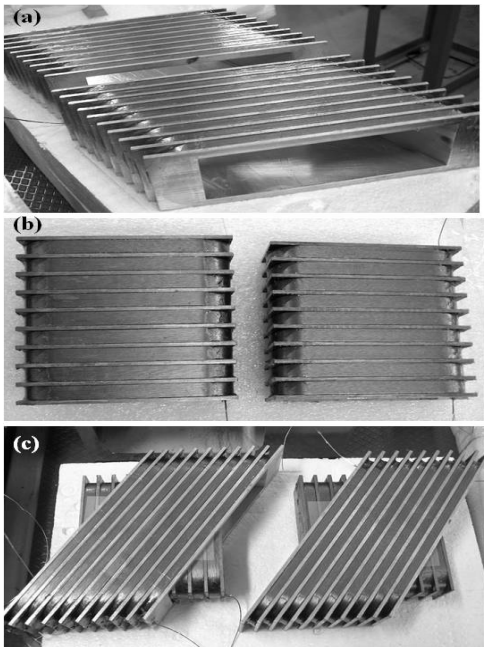

Figure 7. Photographs of (a) outer magnet array with aluminium pole, (b) inner magnet array with iron pole, (c) combined inner and outer magnet arrays.

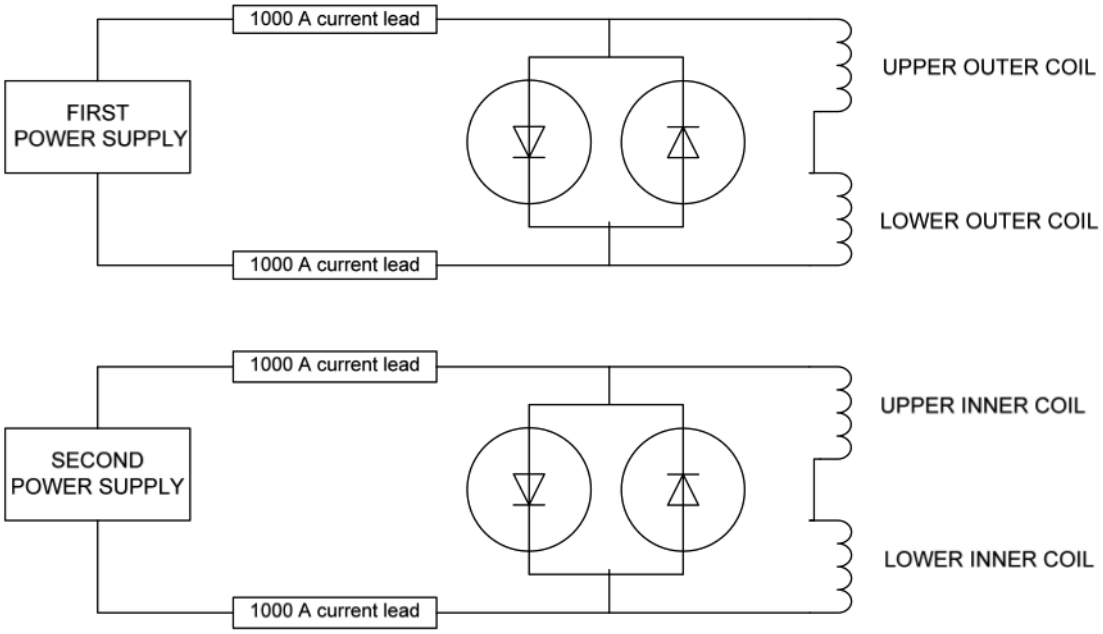

Figure 8. Circuit for quench protection and method of connection of the power supply

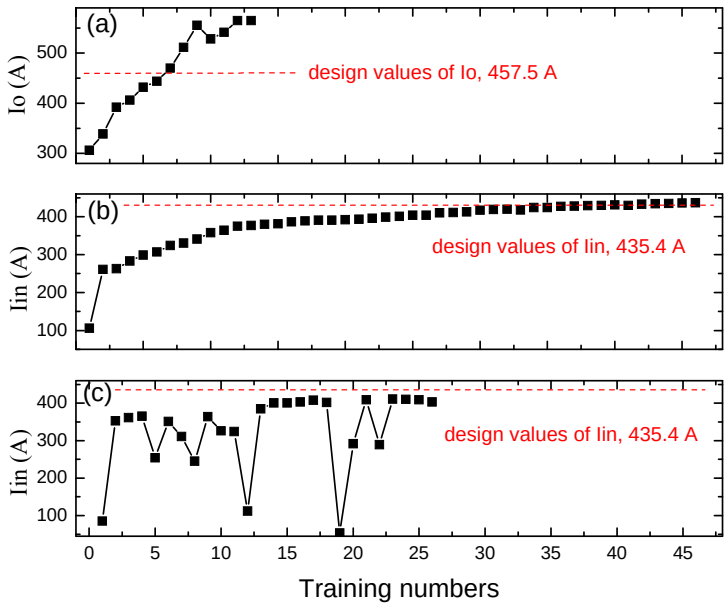

Figure 9. (a) The outer-layer magnet array was trained thirteen times to attain 565 A with $I_i = 0\ A$, (b) the inner-layer magnet array was trained forty-six times to attain 437 A under $I_o = 0\ A$, (c) the inner layer magnet array was trained twenty-six times under I_o= 449 A. Under condition (c), the maximum current of the inner-layer magnet array is 411 A.

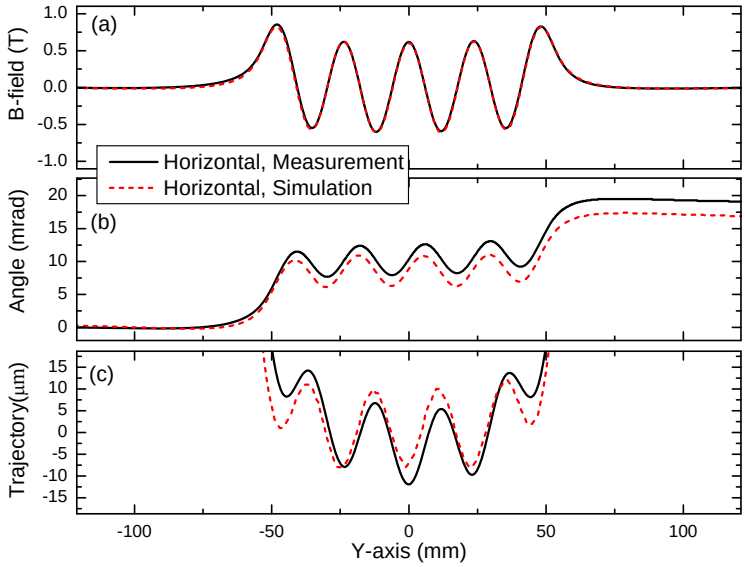

Figure 10. (a) Horizontal field of the distribution of the circularly polarized field on the longitudinal axis was measured with excitation current 449 A in the outer and 380 A in the inner magnet arrays, respectively. The first and second integral fields of the measured field in the test dewar are shown in (b) and (c), respectively. All these were compared with the simulation results in Figure 3.

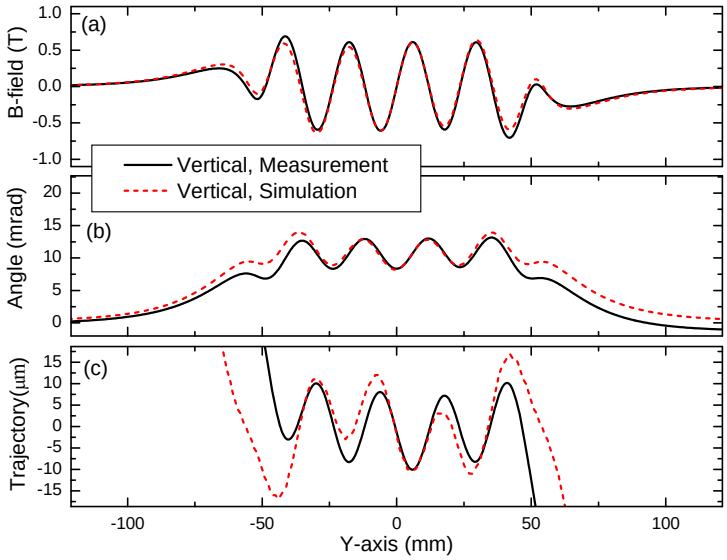

Figure 11. As Figure 10, vertical fields are also drawn.

The outer magnet array was trained first. The excitation current I_o was excited to 565 A with thirteen quenches, as shown in Figure 9(a). The nominal current I_o was 458 A in the outer magnet array, which is 81 % of 565 A. Figure 9(b) reveals that the inner magnet array was trained 46 times and the excitation current I_{in} attained 437 A. When the inner and outer magnet arrays were excited simultaneously, the maximum current of the inner magnet array decreased to 411 A (Figure 9(c)), which is 5.8 % less than the nominal current 435 A. The excitation current was unstable when I_o and I_{in} were both charged rapidly. Therefore, the charging rate was decreased, at least thirty minutes was required for each charging process, to prevent quenching occurring at any current. Both outer and inner magnet arrays can be charged simultaneously; the excitation currents were I_o = 452 A and I_{in} = 411 A. The excitation currents I_{in} and I_o of the circular polarization mode were chosen to be 380 A and 449 A, respectively, for the field measurement; this excitation current was 17 % less than the critical current. In this condition, the helical field was obtained as B_z=B_x=0.61 T. Figure 10(a) and 11(a) show plots of the field distribution, measured with a cryogenic-Hall probe, along the longitudinal trajectory. The electron angle and the trajectory were calculated from the field distribution also shown in Figure 10(b), 10(c), 11(b) and 11(c). The electron angle and the trajectory were adjusted by means of the field of a virtual corrector magnet. This helical field can radiate photons at wavelength 13.5 nm in the 0.8 GeV storage ring and the photon energy is tunable about 13.5 nm on adjusting the excitation current.

5. Conclusion

Because the roll-off of the helical field varied rapidly along the transverse axis, especially at the entrance and exit of the SEPU24, the requirements of highly precise magnet alignment and a high performance of the injection scheme for top-up operation is important. A multipole corrector magnet must be installed at both sides of SEPU24 to steer the orbit of the electrons. The SEPU24 with circular polarization mode can provide highly efficient in-band power for EUV lithography. The generation of variable polarization in SEPU24 becomes possible on combining varied excitation currents. To obtain an intense helical field, the poles of the outer and inner magnet arrays are rotated and fixed, respectively. If polarization must be switched between all polarization modes and the circular polarization mode is not emphasized, the poles of the outer and inner magnet arrays should, however, be interchanged. The 10-pole prototype test indicated that the design and construction of SEPU is consistent; consequently, the mechanism of the superconducting elliptically polarized undulator with the fundamental energy can be developed as a light source for EUV lithography.

Acknowledgments

We thank Mr. Y. C. Fann for assistance with the coil winding. Dr. J. C. Huang, Mr. H. H. Chen, F. Y. Lin and M. H. Huang provided technical discussion and support, and Mrs. P. H. Lin supported data processing and analysis.

References

[1] Guiseppe Dattoli et al. 2001 Extreme ultraviolet (EUV) sources for lithography based on

synchrotron radiation *Nucl. Instrum. Methods Phys. Res., Sect . A* **474** p 259

[2] K Halback 1981 Physical and optical properties of rare earth cobalt magnets *Nucl. Instrum. Methods Phys. Res., Sect.* **187** p 109

[3] S Sasaki 1994 Analysis for a planar variable-polarizing undulator *Nucl. Instrum. Methods Phys. Res., Sect. A* **347** p 83

[4] R PWalker and B Diviacco 1992 Studies of insertion devices for producing circularly polarized radiation with variable helicity in ELETTRA *Rev. Sci. Instrum.* **63** p 332

[5] S Chouhan, DA Harder, G Rakowsky and J Skaritka 2005 Research and Development of a Variable Polarisation Superconducting Undulator at the NSLS *Proceedings of 2005 Particle Accelerator Conference*

[6] A Bernhard, S Chouhan and B Kostka 2005 Superconductive undulators with variable polarization direction *IEEE transactions on applied superconductivity, Vol.* **15***,* No. 2

[7] Proc. Workshop on Superconducting Undulators & Wigglers.Grenoble, 30 Jun.-1st Jul. 2003 available:http://www.esrf.fr/Accelerators/Conferences/ID_Workshop

[8] C S Hwang and P H Lin 2004 Comparison of two superconducting elliptical undulators for generating circularly polarized light *Phys. Rev. ST Accel. Beams Vol.* **7** 090701

[9] R P Walker 2000 New concept for a planar superconducting helical undulator *ELETTRA internal report, Oct.* 20, 2000 (unpublished)

[10] A Bernhard, B Kostka, R Rossmanith and et al. 2004 Planar and planar helical superconducting undulators for storage rings: state of the art *9th European particle accelerator conference EPAC 2004* p 354

[11] C S Hwang, P H Lin, W P Li, C H Chang and T C Fan 2004 Superconducting undulator with variably polarized light *Proceeding of the 2004 FEL conference* p 501

[12] P Elleaume, O Chubar and J Chavanne 1997 Computing 3D magnetic field from insertion devices *Proceeding of Particle Accelerator Conference PAC97* p 3509

[13] F Y Lin, C S Hwang, H H Chen and C Y Kuo 2008 Design and Fabrication of Multipole Corrector Magnet *11th European particle accelerator conference EPAC 2008* p 2368

[14] C S Hwang, P C Chang, C H Chang, C T Chen, B Wang, T Juang, J Y Chen, and R Wahrer 2000 The design of a compact cryogen-free superconducting wavelength shifter for synchrotron radiation *IEEE Trans. Appl. Supercond.*, **10**, No. 1, p 503